Aggregation kinetics of extended porphyrin and cyanine dye assemblies

R. F. Pasternack

C. Fleming

S. Herring

Julio C. de Paula
Haverford College

Repository Citation

Pasternack, Robert F., et al. "Aggregation kinetics of extended porphyrin and cyanine dye assemblies." Biophysical journal 79.1 (2000): 550-560.

Aggregation Kinetics of Extended Porphyrin and Cyanine Dye Assemblies

Robert F. Pasternack,* Cavan Fleming,* Stephanie Herring,* Peter J. Collings,[†] Julio dePaula,[‡] Gerard DeCastro,[§] and Esther J. Gibbs[§]

*Department of Chemistry, Swarthmore College, Swarthmore Pennsylvania 19081; [†]Department of Physics and Astronomy, Swarthmore College, Swarthmore, Pennsylvania 19081; [‡]Department of Chemistry, Haverford College, Haverford, Pennsylvania 19041; and [§]Department of Chemistry, Goucher College, Towson, Maryland 21204 USA

ABSTRACT　The kinetics of J-aggregate formation has been studied for two chromophores, tetrakis-4-sulfonatophenylporphine in an acid medium and pseudoisocyanine on a polyvinylsulfonate template. The assembly processes differ both in their sensitivity to initiation protocols and in the reaction profiles they produce. The porphyrin's assembly kinetics, for example, displays an induction period unlike that of the cyanine dye. Two kinetic models are presented. For the porphyrin, an autocatalytic pathway in which the formation of an aggregation nucleus is rate-determining appears to be applicable; for the pseudoisocyanine dye, an equation derived for diffusion-limited aggregation of a fractal object satisfactorily fits the data. These models are shown to be useful for the analysis of kinetic data obtained for several biologically important aggregation processes.

INTRODUCTION

Recent reports from our laboratories have dealt with the spontaneous self-association of porphyrins and chlorins to form molecular assemblies, both with and without added polymeric templates (Pasternack et al., 1994, 1998a; de-Paula et al., 1995). These studies are intended, in part, to contribute to a general understanding of noncovalently based supramolecular organizations, so prevalent in biological systems. In the course of these investigations, the usefulness of resonance light scattering (RLS) in complementing absorption (extinction) and circular dichroism measurements for the detection and characterization of extended, electronically coupled chromophore assemblies has been demonstrated (Pasternack et al., 1993, 1994, 1998b; dePaula et al., 1995; Pasternack and Collings, 1995; Parkash et al., 1998). Among the systems considered thus far are aggregates of the diacid form of several sulfonatophenylporphines (Pasternack et al., 1994) and the cationic *trans*-H_2Pagg porphyrin (structures are shown in Fig. 1), in both the absence and presence of DNA or polyglutamate biopolymers (Pasternack et al., 1993; Pasternack and Gibbs, 1993). In addition to spectroscopic and thermodynamic studies, we have reported on the kinetics of formation of one such very large assembly (*trans*-H_2Pagg on a DNA template; Pasternack et al., 1998a). In the present paper we extend our kinetics studies to include assembly formation of two J-aggregates; one a porphyrin in the absence of a template and the other a noncyclic chromophore, pseudoisocyanine, on polyvinylsulfonate.

J-aggregates, first described by Jelley and Scheibe in 1936 (Jelley, 1936; Scheibe, 1936) for cyanine dyes, are molecular arrays in which the slip angle, that is, the angle between the molecular long axis and the line of centers of stacked molecules, is appreciably less than 90°. The electronic coupling of the monomers of a J-aggregate result in a characteristic narrow, red-shifted extinction band. The solution properties of one such dye, 1,1′-diethyl-2,2′-cyanine (pseudoisocyanine, PIC^+, Fig. 1) chloride have been studied extensively, and evidence has been provided for aggregates whose size has been estimated to be anywhere from tens of monomer units to several hundreds or thousands of units (Sundstrom et al., 1988; Horng and Quitevis, 1993; Makio et al., 1980; Maiti et al., 1995; Ohno et al., 1993). The formation of the aggregate can be accomplished by any of a number of approaches, including high dye concentration (millimolar range) or, at micromolar concentrations, raising the electrolyte (sodium chloride) concentration to 5–6 M, or through the addition of certain anionic polymers, such as polyvinylsulfonate (PVS) (Fig. 1). The pseudoisocyanine J-aggregate displays an intense narrow extinction band at ~567–570, the exact position of which depends somewhat on solution conditions and the method of aggregate preparation. Unlike many other systems, PIC^+ aggregates have a higher quantum yield for fluorescence ($\phi \approx 0.022$ on a PVS template) than its monomer, with little if any Stokes shift (Horng and Quitevis, 1993). The position and intensity of the fluorescence have made interpretation of RLS experiments on the aggregate problematic at best. In this paper, we describe a strategy for detecting RLS signals in the presence of fluorescence emission and confirm that PIC^+ forms an extended aggregate in solution when bound to PVS by demonstrating the existence of an enhanced RLS signal for this system.

By comparison, RLS measurements on porphyrin assemblies have generally been straightforward. The diacid forms of two 4-sulfonatoporphines, $H_4TPPS_3^-$ and $H_4TPPS_4^{2-}$, for
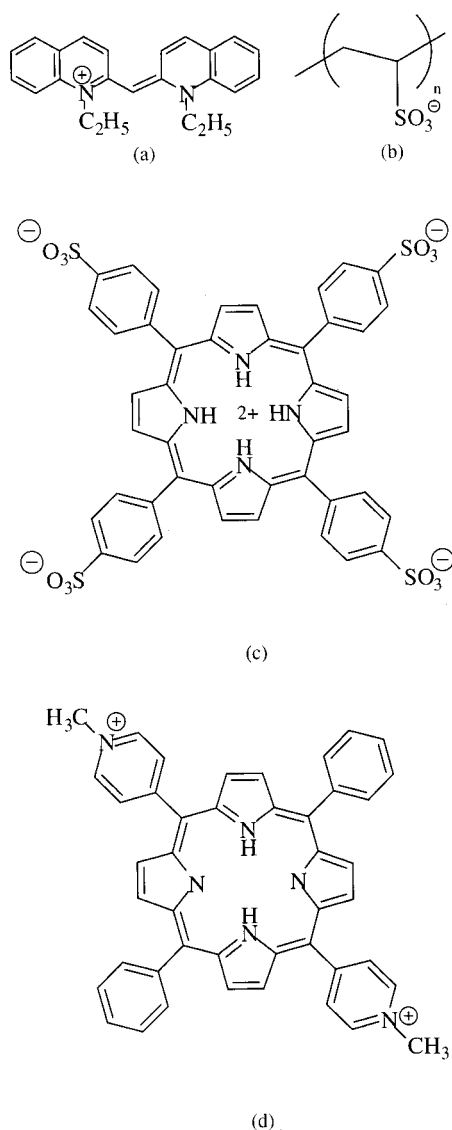

FIGURE 1 Structures of the reactants. (*a*) Pseudoisocyanine (PIC$^+$). (*b*) Polyvinylsulfonate (PVS). (*c*) The diacid form of tetrakis-4-sulfonatophenylporphine (H$_4$TPPS$_4^{2-}$). And, for comparison, (*d*) the free-base form of *trans*-bis(*N*-methylpyridinium-4-yl)diphenylporphine (trans-H$_2$Pagg).

example, show markedly enhanced scattering signals in both the Soret and Q-band regions (Pasternack et al., 1994). Studies of the aggregation properties of these two sulfonated derivatives of tetraphenylporphine began over 25 years ago, when Fleischer et al. (1971) and Pasternack et al. (1972) independently reported the formation of an unusually narrow band of Soret intensity near 490 nm, suggested as arising from the aggregation of the diacid form of the porphyrin. The monomer Soret band of H$_4$TPPS$_3^-$ or H$_4$TPPS$_4^{2-}$ is observed near 435 nm when the pH is lowered below the pK$_a$ of the porphyrins, ~4.8 (Fleischer et al., 1971; Pasternack et al., 1972). However, as the pH is lowered still further to ~1, a new, "anomalous," extremely

narrow band at 490 nm is observed, now known to be due to the formation of a J-aggregate. In the years since these first reports, a large number of studies on these porphyrin derivatives have appeared, such as methods to induce the diacids to aggregate at somewhat higher pH by increasing the ionic strength and/or including a surfactant (Maiti et al., 1995, 1998). A variety of physical measurements have been performed on these porphyrin J-aggregates, including our studies on enhanced Rayleigh scattering at 490 nm and the determination of their size from RLS and static light scattering experiments (Pasternack et al., 1994; Maiti et al., 1995, 1998; Ohno et al., 1993; Collings et al., 1999; Akins et al., 1994; Ribo et al., 1994; Rubires et al., 1999). These aggregates prove to be very large, involving tens to hundreds of thousands of monomer units (Pasternack et al., 1994; Collings et al., 1999). In the present paper we report on the kinetics of assembly formation of H$_4$TPPS$_4^{2-}$ and compare the results to those obtained for PIC$^+$ in the presence of PVS. The features of the kinetic behaviors observed for these J-aggregate-forming chromophores are shown to parallel the characteristics obtained by others for biologically relevant aggregation processes.

MATERIALS AND METHODS

Porphyrin system

The porphyrin (tetrakis-4-sulfonatophenyl)porphine (Fig. 1) was purchased from MidCentury Chemical as the sodium salt. Stock porphyrin solutions were passed through 0.2-μm Nalgene filters within a few hours before use. Porphyrin concentrations were determined in 0.1 mM phosphate buffer (pH 6.8), using $\epsilon = 5.33 \times 10^5$ M^{-1} cm^{-1} at the Soret maximum at 413 nm for the free-base form (Fleischer et al., 1971). The porphyrin solutions for kinetic analyses were prepared such that the final HCl concentration was always 0.3 M (pH ~0.5). Mixing of the free-base form of the porphyrin with the acid was carried out by two distinct protocols. In method I, a small volume of a concentrated porphyrin stock was added to an acid medium (HCl) with the use of a micropipette. In method II, the porphyrin stock was first diluted with water and then added to an equal volume of an HCl solution. A series of kinetic experiments were conducted over a porphyrin concentration range of 3–7 μM, using method II with constant stirring. Extinction versus time scans were obtained at both 435 nm (Soret band of the diacid monomer) and 490 nm (Soret band of the J-aggregate). The temperature was maintained at 25°C.

Pseudoisocyanine/polyvinylsulfonate system

Pseudoisocyanine (PIC$^+$) was purchased from Sigma as the iodide salt, dissolved in methanol, and converted to the chloride form by ion exchange chromatography. The chloride stock solution was then passed through a 0.2-μm filter and found to be stable for up to 2 weeks if kept in the dark. Concentrations of the dye stock were determined using an ϵ_{520} of 6.0×10^4 M^{-1} cm^{-1} (Norden, 1977). Solutions prepared from stock for kinetic runs contained between 1% and 3% methanol. Care must be taken to avoid too much methanol in working solutions, as alcohol inhibits aggregation of the dye.

PVS as the sodium salt was purchased from Aldrich (25% by weight in water), purified by a published procedure (Horng and Quitevis, 1993), and stored in a desiccator. Concentrations were determined by mass, using 130.1g/mol for the repeat unit. Stock solutions of PVS were not filtered.

PIC$^+$ solutions for kinetic studies of the aggregation process were prepared via the two protocols described earlier for the porphyrin system. In method I, a small volume of a concentrated PIC$^+$ stock was added to either a PVS or a NaCl solution (the aggregating media) with a micropipette. In method II, the PIC$^+$ stock was diluted with water and then added to an equal volume of a PVS solution (solubility considerations preclude using this method for NaCl-induced aggregation). Extinction versus time scans were obtained at the aggregate maximum, which varied from ~566 to 568 nm, depending on the concentration of the aggregate and other solution conditions. Color changes at the monomer peaks were relatively small and were not monitored for kinetic analysis. The temperature was maintained at 25°C. A few of the kinetic experiments were conducted with continuous stirring, but most were left unstirred after the initial mixing procedure. The kinetic data for the PIC$^+$/PVS system showed small variations from run to run, so the analyses for three separate experiments were averaged for each solution condition. The most reproducible data were obtained with method II and a 1:1 ratio of dye and polymer, without stirring. The concentration range studied was from 10 to 20 μM dye and polymer.

General information

All other chemicals were purchased from Fisher Scientific and were used without further purification. Millipore-purified water was passed through a 0.2-μm Nalgene filter before use in the preparation of solutions. The porphyrin and PIC$^+$ stock solutions, prepared in glass vials, were stored in the dark and used within 2 weeks. Reaction solutions were generally prepared and measured in methacrylate cuvettes, assuming volumes to be additive.

Extinction spectra and kinetic data were obtained with a Jasco V-550 UV/vis spectrophotometer. Stopped-flow kinetic data were obtained with a Durrum model D-110 instrument. Fluorescence and resonance light scattering experiments were performed with a Fluorolog III spectrofluorimeter with signal intensities reported as sample/reference. In some cases, especially those requiring the measurement of scattering intensity as a function of angle from the exciting beam, a Coherent Innova 70 mixed gas laser (argon and krypton), equipped with a Brookhaven Instrument Corporation BI-200SM goniometer and PMT detector, was employed. All fluorescence and RLS detection wavelengths refer to the central wavelength of the 10-nm bandpass filters utilized. Data extracted from literature figures were obtained by scanning on an Apple ColorOneScanner using Scantastic software. Data points from the PICT files were obtained using a GraphicConverter program. Kinetic data were analyzed using Kaleidagraph software.

It should be emphasized that "absorption" measurements of the aggregates in these systems show appreciable scattering (both on- and off-resonance) and therefore are more appropriately referred to as extinction measurements. For another aggregating porphyrin system, trans-H$_2$Pagg, the aggregate of which also provides an enhanced RLS spectrum, the intensity of RLS and extinction signals have been shown to increase linearly with increasing concentration of chromophore monomers in the aggregated form (Pasternack et al., 1998b). We have applied this result to the systems being studied here. As confirmation, we find that the kinetic parameters obtained from the analysis of kinetic data for the H$_4$TPPS$_4^{2-}$ system at the monomer peak (435 nm), where there is minimal scattering in the extinction data, are nearly identical to those obtained at the aggregate peak near 490 nm.

RESULTS

Aggregation of H$_4$TPPS$_4^{2-}$ in the presence of 0.3 M HCl

Shown in Fig. 2 are the extinction and RLS spectra, respectively, for solutions of 1.9 μM H$_4$TPPS$_4^{2-}$ at pH 3 and 0.5.
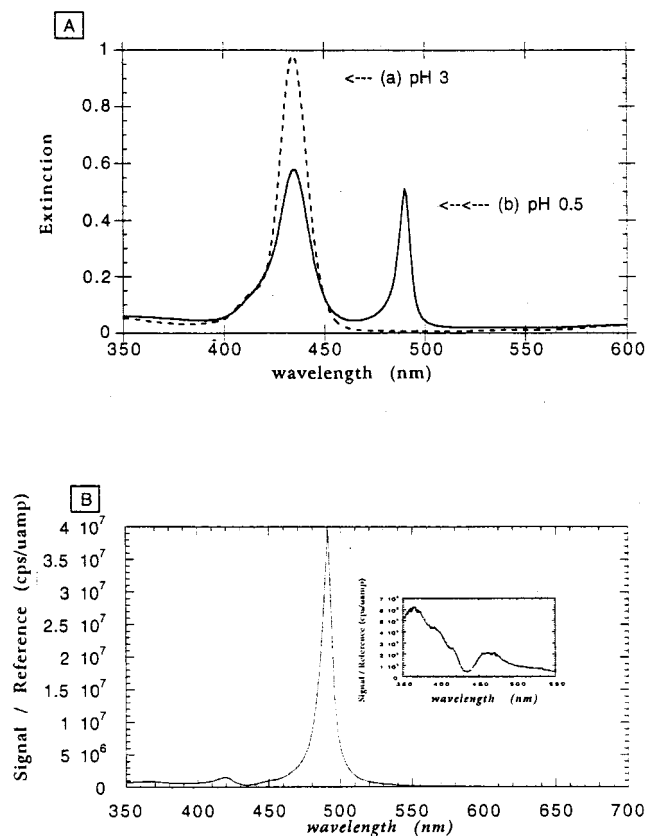

FIGURE 2   (A) Extinction spectra of H$_4$TPPS$_4^{2-}$ solutions at pH 3 (curve a) and pH 0.5 (curve b). The monomer Soret band of the diacid form of the porphyrin is at 435 nm; the J-aggregate produces a band of Soret intensity at 490 nm. (B) Resonance light scattering spectra of the solutions of A. The aggregate produces a markedly enhanced RLS signal at 490 nm, a small trough at 435 nm, and a smaller enhanced RLS signal near 420 nm, whereas the monomer (inset) shows only a trough at 435 nm.

At pH 3, the diacid porphyrin is monomeric and has its Soret absorption maximum at 435 nm. The RLS spectrum of the diacid monomer (best seen in the inset of Fig. 2 B) contains no peak maxima, but rather a small decrease from the background Rayleigh scattering near 435 nm due to absorption effects. When the pH of the H$_4$TPPS$_4^{2-}$ solution is lowered to pH 0.5, some of the diacid monomers assemble to form J-aggregates, and a new extinction band at 490 nm appears. For this same porphyrin solution at pH 0.5, the RLS spectrum has an intense peak with its maximum at 490 nm, the position in the extinction spectrum for the J-aggregate. No RLS peak at 435 nm—the position of the absorbance band for the porphyrin diacid monomer—is present, only a small trough in the signal due to absorption effects. A small RLS peak is observed slightly to the blue of the 435-nm feature, which may be due to an H-aggregate (slip angle = 90°) previously reported for this porphyrin (Maiti et al., 1998).

Presented in Fig. 3 are three kinetic profiles for the conversion of the diacid monomeric form of the H$_4$TPPS$_4^{2-}$ porphyrin to a J-aggregate. Aggregate formation was initi-
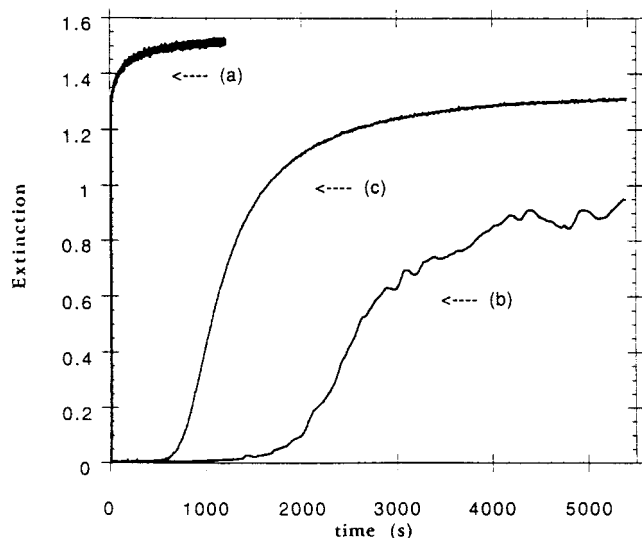
FIGURE 3   Reaction profiles for the aggregation of three $H_4TPPS_4^{2-}$ solutions differing only in the protocol of mixing. See Materials and Methods for details. (*a*) Mixing method I. (*b*) Mixing method II, no stirring. (*c*) Mixing method II with stirring.

aggregates grows slowly over extended time periods, but if the solution is agitated (stirred or inverted) the size returns to a smaller value (Collings et al., 1999). We were able to eliminate these higher order structures in the kinetic runs by gentle stirring of the solution over the course of the reaction (Fig. 3 *c*). It was observed that stirring also has the effect of shortening the "incubation" period and generally speeding up the aggregation. For all of the kinetic data analyzed and described, method II was used for sample preparation, and the solutions were continuously stirred during the course of the reaction. Over the concentration range studied, 3–7 μM, this protocol provided reproducible kinetic profiles. All of the kinetic profiles showed three general regions, as displayed in Fig. 3 *c*: an initial "delay or lag" period, followed by rapid formation of ~80–85% of the aggregate, and, finally, a slow approach to the equilibrium position.

Aggregation of PIC^+ on the PVS polymer template

Shown in Fig. 4 *A* are the extinction spectra of 10 μM PIC^+ dye with and without the addition of an equal concentration
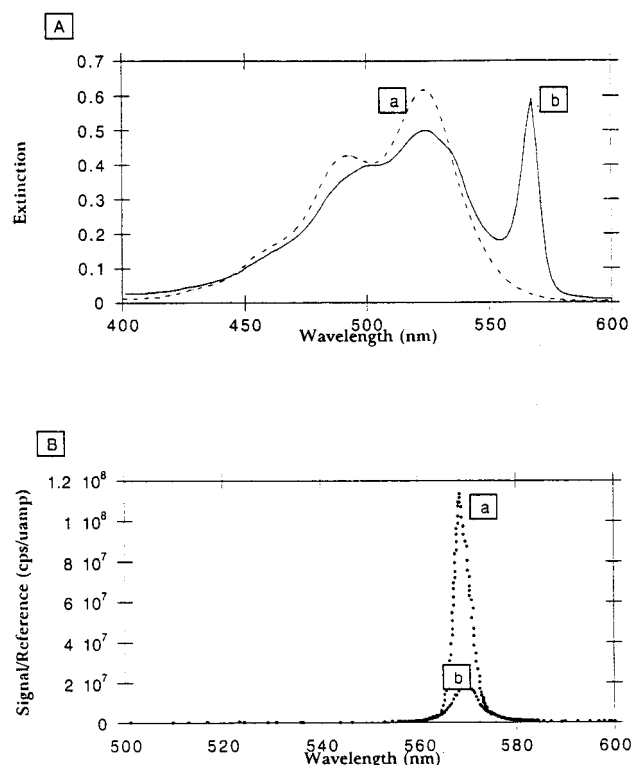
ated via the addition of HCl to a near-neutral porphyrin solution. The kinetics of the aggregation process were monitored at the 490-nm product peak by extinction spectroscopy. The final solution conditions for each kinetic profile are 4.5 μM porphyrin and 0.3 M HCl. The striking differences among the profiles lay in the specifics of the experimental protocol used for mixing reagents (see Materials and Methods) (Fig. 3, curves *a* and *b*; compare mixing via methods I and II). Mixing method I (Fig. 3 *a*) involves the addition of a highly concentrated porphyrin solution (~0.1 mM) to the HCl medium. This protocol leads to kinetics that are too rapid to follow by ordinary methods; over 85% of the initial extinction change is missed in the ~10 s required to mix reagents in the cuvette and place the sample in the housing of the spectrophotometer. However, using a protocol (method II) in which the concentration of the porphyrin solution added to the aggregation medium is considerably lower (micromolar range) leads to aggregation kinetics that are significantly slower, although the final concentration of porphyrin after mixing is the same for the two experiments. The extinction at the start of the reaction, when followed at the product peak, is zero within experimental error, and therefore the total extinction change could be monitored. However, an additional complication arises; the time-dependent extinction curve for method II is not smooth, but rather displays somewhat chaotic rises and falls superimposed on the reaction profile. We interpret these effects as being due to the formation of rather fragile aggregation networks, i.e., higher order assemblies involving interactions of aggregates. In static and dynamic light scattering experiments, we have observed that the apparent size of the

FIGURE 4   (*A*) Extinction spectra of 10 μM PIC^+ (*a*) without and (*b*) in the presence of an equal concentration of PVS. (*B*) *Curve a*: Signal obtained for a PIC^+/PVS solution from an "RLS-type" experiment (synchronous scanning with both monochromators preset to an identical wavelength). *Curve b*: Signal obtained for the same solution with an emission scan protocol with excitation at 454 nm.

of PVS polymer. In the absence of PVS, the dye is mono-meric and displays a broad absorption envelope between 450 and 550 nm (Fig. 4 *A, spectrum a*). No RLS peaks are observed for solutions of PIC^+ monomers in water over a scanning range of 400–700 nm; only small dips appear in the background Rayleigh scattering due to absorption. Upon the addition of PVS, the monomer absorption envelope decreases in intensity, with the appearance of a narrow band at ~568 nm (see Fig. 4 *A, curve b*). In the presence of the PVS template, the "RLS-type experiment" (synchronous scanning of the two monochromators preset to an identical wavelength) displays a narrow peak at ~568 nm (see Fig. 4 *B*), the same wavelength at which the new peak due to the J-aggregate appears in the extinction spectrum. However, it should be pointed out that the basis for the feature detected in the RLS-type experiment is not as straightforward here as for porphyrin systems because of fluorescence contribu-tions. The exact position of the J-aggregate peak maximum varies slightly, depending on the concentration of J-aggre-gate, the ratio of dye to polymer, and solution conditions (Horng and Quitevis, 1993). The addition of 10 mM NaCl to solutions of PIC^+ and PVS causes the J-aggregate peak at 568 nm to disappear in extinction and RLS-type experi-ments. This observation indicates the reversibility of the aggregation process and the extreme sensitivity of the equi-librium to ionic strength.

Fluorescence emission spectral experiments for solutions of 60 μM PIC^+ monomers in water and in dimethyl sul-foxide were obtained. Using an excitation wavelength of 495 nm, we find that the emission spectra in the two solvent systems show an extremely weak and broad fluorescence peak from ~540 nm to 600 nm. The results of emission and RLS-type experiments for a solution at 10 mM PIC^+ and 90 μM PVS, which contains both monomers and J-aggregates, are shown in Fig. 4 *B*. When an excitation wavelength of 454 nm is employed, a narrow fluorescence peak, at least two orders of magnitude more intense than the fluorescence peak for solutions containing only monomer, is observed (Fig. 4 *B, spectrum b*). The peak maximum is at 568 nm, again at the same wavelength as the extinction peak ob-served for the J-aggregate. The characteristics of this spec-trum—the large fluorescence intensity, the narrowness, and the position of peak maximum—as compared to the solution with only monomer, indicate that the fluorescence is due primarily to the J-aggregate, not to the monomers also present in the solution. An excitation spectrum of this same solution, with detection at 568 nm, was examined. Two excitation peaks, at ~495 nm and ~530 nm, are observed. If the intensity at a detection wavelength of 568 nm were due exclusively to enhanced RLS, features at shorter wave-lengths would not appear. To summarize these findings: 1) unlike the general pattern observed for most porphyrin aggregates, J-aggregates of PIC^+ fluoresce with a greater quantum efficiency than the monomer units; and 2) there

appears to be little or no Stokes shift of the fluorescence peak of the PIC^+ J-aggregate.

Because the fluorescence peak of the J-aggregates of PIC^+ displays virtually no Stokes shift, the question re-mains: How much of the "RLS spectrum" of the J-aggre-gates is due to fluorescence and how much, if any, is due to true RLS enhancement? To address this question, advantage is taken of the difference in the angular dependence of RLS and fluorescence signals. The fluorescence signal intensity in solution is expected to be independent of the angle of detection, whereas scattering signals have a distinct angular dependence reflecting the size and structure of the aggregate (Collings et al., 1999). Experiments to measure scattering intensity as a function of angle were therefore undertaken, using the laser apparatus described previously. As a refer-ence point, the emission from a solution of ZnTMpyP—a metalloporphyrin that does not aggregate under the concen-tration conditions used here (Pasternack et al., 1973)—was studied. The metalloporphyrin was excited at 454 nm (near its Soret wavelength absorption maximum), and its fluores-cence was monitored at 650 nm (near its fluorescence maximum), and no dependence of fluorescence intensity on detection angle was observed (Fig. 5 *a*). On the other hand, when the scattering as a function of angle at an excitation and detection wavelength of 650 nm (where there are no absorption bands) was measured for a solution containing PIC^+ as a mixture of monomers and J-aggregate (10 μM PIC^+ and PVS), the "normal" or nonresonance scattering intensity varied with detection angle (see Fig. 5 *b*). For a solution containing PIC^+ aggregates and monomers, excit-ing at 454 nm and detecting at 570 nm, a wavelength combination that is dominated by fluorescence, produces
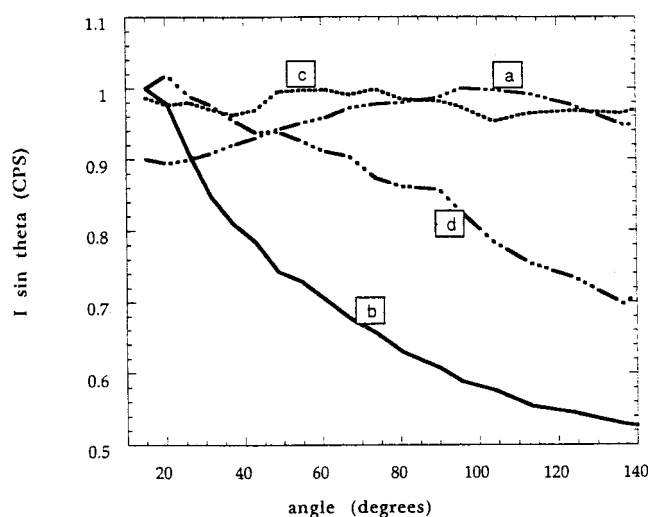

FIGURE 5 Angular dependence of scattering/fluorescence signals. (*a*) Fluorescence of ZnTMpyP. (*b*) Off-resonance scattering by PIC^+ aggre-gates. (*c*) Fluorescence of PIC^+ aggregates. (*d*) Combination of fluores-cence and resonance scattering by PIC^+ aggregates. Each profile has been normalized to an average maximum value of unity.

signals whose intensity is constant as a function of angle (see Fig. 5 c). But, as seen in Fig. 5 d for a solution containing PIC^+ aggregates and monomers, using an excitation and detection wavelength of 570 nm—the wavelength of the extinction and fluorescence maxima—produces signals whose intensity varies with angle of detection superimposed upon a constant background. This indicates that a significant RLS enhancement exists for these aggregates in addition to the fluorescence signal. As a rough estimate, the RLS signal is comparable to the fluorescence intensity.

As shown in Fig. 6, kinetic profiles produced by adding equimolar amounts of PVS polymer to the PIC^+ dye and monitored at the extinction peak for the J-aggregate do not have the initial delay or lag period observed for the $H_4TPPS_4^{2-}$ system (compare to Fig. 3). At the higher concentration end of the range considered, a substantial portion of the extinction change is missed via hand-mixing of solutions. The stopped-flow technique was applied, in which the mixing is complete within 5 ms; all of the extinction change is now observed. Still, there is no indication of a lag or incubation period. Furthermore, the PIC^+/PVS system is not nearly as sensitive to mixing protocol as is the $H_4TPPS_4^{2-}$ system. For PIC^+, the two mixing methods described earlier give similar results, i.e., when equal volumes of PVS and PIC^+ are mixed by turbulent flow (by rapid injection into a beaker using syringes), the results are almost identical to those obtained by simple pouring together of the two solutions. The formation of transient species (see Fig. 3 b) during the course of the kinetic process, as seen for $H_4TPPS_4^{2-}$, was not observed for the PIC^+ aggregation, and continuous stirring during kinetic runs did not have a discernible effect on the kinetic pattern.
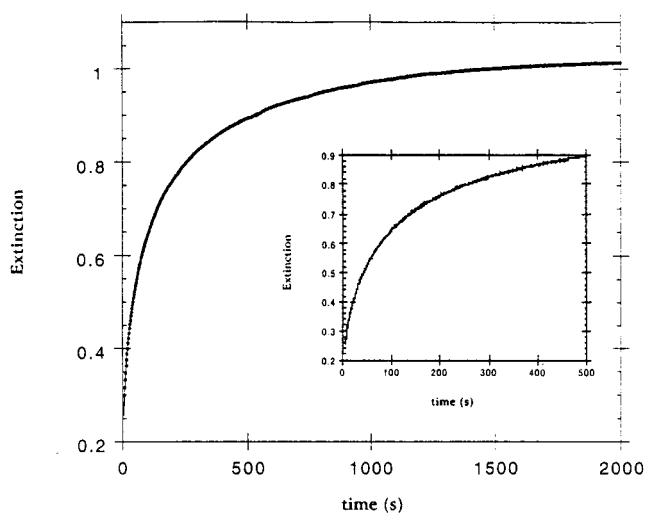

FIGURE 6 Kinetic profile obtained for the aggregation of PIC^+. Both the data (*small circles*) and fit (*continuous line*) to Eq. 5 are shown. The inset emphasizes the early portion of the kinetic profile to demonstrate the absence of any systematic deviation in the region most sensitive to the model.

A variety of $[PVS]/[PIC^+]$ values were investigated, but the most nearly reproducible results were obtained for the 1:1 ratio. Therefore, as described earlier, all kinetic runs for the PIC^+/PVS system employed simple hand mixing of solutions without turbulent flow (except for those using the stopped-flow technique), the solutions were not stirred during the course of the aggregation process, a $[PVS]/[PIC^+] = 1$ was maintained, and at least three runs at a given set of conditions were averaged. Kinetic data were obtained in a concentration range of 10–20 μM, limited by the extreme sensitivity of the extent of aggregation and of the reaction rate to concentration. At concentrations lower than 10 μM, there is very little aggregation and thus there are small changes in extinction; at concentrations greater than 20 μM the kinetics become quite rapid and values for the extinction become large and are subject to significant error.

ANALYSIS AND DISCUSSION OF KINETIC DATA

Aggregation of PIC^+ on the PVS polymer template

Because kinetic data for the PIC^+/PVS and porphyrin/HCl systems could not be successfully fit by standard methodologies (e.g., first-order, second-order, or coupled first-order), our analysis takes a less conventional approach. It has been shown that for self-similar systems, rate constants are time dependent, and the mean aggregate size, $s(t)$, scales as a power law dependence on time, $s(t) \approx t^n$ (Leyvraz, 1986). In the case of a diffusion-limited aggregation (DLA) process, it has been shown (Leyvraz, 1986) that for nongelling systems in which larger clusters grow primarily by reaction with smaller clusters, a monodispersed system is rapidly generated. Under such conditions the free monomer concentration decreases exponentially as a power of time (sometimes referred to as a "stretched exponential" dependence). Taking into account the reversibility of the reaction, the following equation results:

$$([M] - [M]_\infty) = ([M]_0 - [M]_\infty)\exp(-(kt)^n) \quad (1)$$

where $[M]$ is the free monomer concentration at time t, $[M]_0$ is the initial total concentration of monomer units, and $[M]_\infty$ is the concentration of free monomer units at equilibrium. A monodispersed, nongelling system such as the one being considered here requires that $n < 1$ (Leyvraz, 1986).

For the PIC^+/PVS system, the small changes in extinction in the monomer region limit monitoring of the reaction to the region of the spectrum near the aggregate peak (~565 nm). If the concentration of aggregate is defined in terms of the concentration of aggregated (monomeric chromophore) units and no aggregates are present at $t = 0$, then, for a two-state system,

$$[M]_0 = [M] + [Agg] \quad (2)$$

$$[Agg] = ([M]_0 - [M]_\infty)\{1 - \exp(-(kt)^n)\} \quad (3)$$

Because the kinetics are followed with an absorbance spectrometer, it is extinction that is measured at the aggregate peak. Therefore,

$$\text{Ext}_t = \varepsilon_M[M]_t + \varepsilon_{Agg}[Agg]_t \quad (4)$$

and

$$\text{Ext} = \text{Ext}_0 + \{(\text{Ext}_\infty - \text{Ext}_0)[1 - \exp(-(kt)^n)]\} \quad (5)$$

Kinetic data were obtained for five sets of conditions at $[PIC^+] = [PVS]$ over the concentration range of 10–20 μM. Shown in Fig. 6 is the best fit of the data obtained at 15 μM of reactants, using Eq. 5. The quality of fit is quite good, with an R^2 value of 0.9997. The inset in Fig. 6 presents the data and calculated curve for the first part of the kinetic profile, demonstrating the quality of fit in this region. Shown in Table 1 below is a summary of the parameters obtained for the five sets of conditions using this model. The agreement of the parameters for repeated trials is within $\pm 25\%$ of the average values. For the two highest concentration solutions, 17.5 and 20 μM, kinetic data were obtained using hand-mixing and stopped-flow techniques because, for these solutions, the reactions are sufficiently fast that a major part of the extinction change is lost in the hand-mixing technique. Values for k and n given in the table for these conditions represent a weighted average of stopped-flow and hand-mixing protocols. Reasonably good agreement was obtained for the two kinetic methods. For example, at 17.5 μM, hand-mixing gave average values of $k = 0.081$ s^{-1} and $n = 0.33$, whereas the stopped-flow method gave average values of $k = 0.11$ s^{-1} and $n = 0.39$. The rate constant, k, shows a very sensitive dependence on the initial concentration of reactants; a plot of ln k against the initial concentration of reactants is linear, leading to an empirical equation of the form $k \approx 6.3 \times 10^{-6} \exp(5.5 \times 10^5 [PIC^+]_0)$. The value of n, on the other hand, is not nearly as sensitive to concentration. A plot of n versus concentration is linear, with the value of n decreasing with increasing concentration. When extrapolated to zero concentration, $n > 0.9$, suggesting that the reaction reverts to a simple first-order process at the lower limit of concentration.

Aggregation of $H_4TPPS_4^{2-}$ in the presence of 0.3 M HCl

As described previously and clearly demonstrated by a comparison of Figs. 6 and 7, the overall kinetic profile for

TABLE 1 Values for rate constant and *n*, from Eq. 5, for the aggregation of PIC$^+$ as induced by PVS polymer

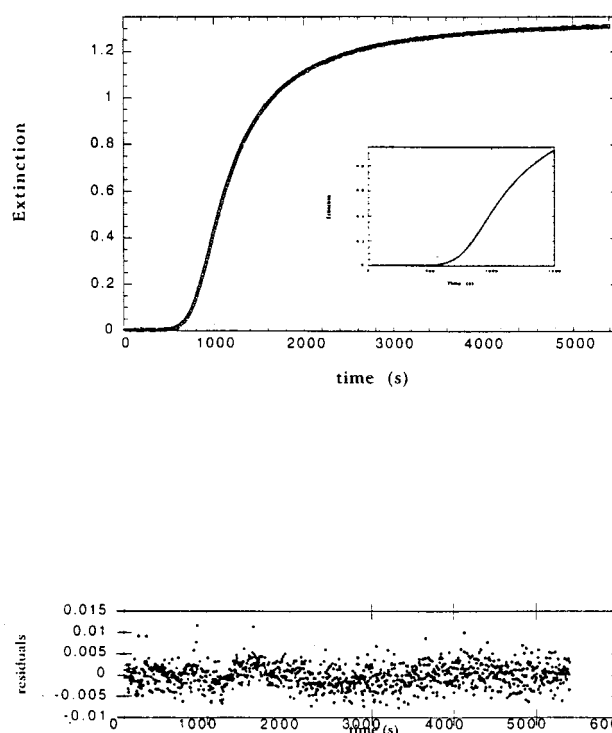| $[PIC^+] = [PVS]$ (μM)	k (s^{-1}) $\times 10^3$	n
10	0.97	0.64
12.5	3.1	0.45
15	8.6	0.46
17.5	100	0.37
20	360	0.30

FIGURE 7 Kinetic profile obtained for the aggregation of $H_4TPPS_4^{2-}$. Both the data (*small circles*) and fit (*continuous line*) to Eq. 6 are shown. The inset emphasizes the early portion of the kinetic profile to demonstrate the absence of any systematic deviation in the region most sensitive to the model. The residuals, shown at the bottom of the figure, further confirm the high quality of the fit of the data by the present model.

$H_4TPPS_4^{2-}$ aggregation is quite different from that for the aggregation of PIC$^+$. Most prominent is the delay or lag period observed for the porphyrin system. When the data for the aggregation of $H_4TPPS_4^{2-}$ in the presence of 0.3 M HCl are analyzed using Eq. 5, the quality of the fit is poor. Instead, a kinetic model was employed that we had previously suggested (Pasternack et al., 1998a) for the autocatalyzed formation of organized assemblies of DNA-bound porphyrins. The model is derived for a process in which the porphyrin assembly catalyzes the rate-limiting step in the aggregation process. In a sense, this mechanism can be considered as a form of surface catalysis, with the rate constant dependent on the extent of the surface. However, in the present case, the "surface" (i.e., the porphyrin assembly) grows with time. Thus the experimental rate constant is itself time-dependent. The expression derived earlier for this model is

$$([M] - [M]_\infty)/([M]_0 - [M]_\infty)$$
$$= (1 + (m - 1)\{k_0 t + (n + 1)^{-1}(k_c t)^{n+1}\})^{-1/(m-1)} \quad (6)$$

The four kinetic parameters that appear in Eq. 6 are k_0, the rate constant for the uncatalyzed growth; k_c, the rate constant for the catalytic pathway; n, a parameter that describes

the growth of the chromophore assembly as a power function of time (as proposed by Leyvraz, 1986); and m, which is related to the size of the "critical nucleus," the formation of which is the rate-determining step in the process. The derivation of Eq. 6 requires that m not be equal to 1 (Pasternack et al., 1998a). (It is interesting to note that for the special case where $m = 1$, the derivation leads to a stretched exponential form.) $[M]_0$ is the total porphyrin concentration (expressed in monomer units). We set $([M] - [M]_\infty)/([M]_0 - [M]_\infty) = (Ext - Ext_\infty)/(Ext_0 - Ext_\infty)$ as earlier, where Ext is the extinction of the solution at the selected wavelength. Fig. 7 shows the fit of the kinetic data to this autocatalytic model for the aggregation of $H_4TPPS_4^{2-}$ (at a porphyrin concentration of 4.5 μM) and the residuals calculated for this fit. The inset in this figure examines the data early in the run to emphasize the success of the model in fitting this portion of the kinetic profile. It should be borne in mind that a single set of parameters is used throughout; i.e., no arbitrary parsing of the kinetic profile into different "phases" is performed.

Shown in Table 2 is a summary of the kinetic parameters obtained from an analysis of the kinetic data using Eq. 6, for a concentration range of $H_4TPPS_4^{2-}$ of ~3–7 μM. Where multiple runs were attempted, often with different stock solutions, agreement among the parameters was within ±10%. The extinction data were fit with six parameters, the four kinetic parameters described above, and two extinctions, one for time 0 (Ext_0) and the other at the end of reaction (Ext_∞). In general, the agreement between the best fit and the experimentally measured values for Ext_0 and Ext_∞ was excellent. Where comparisons were made, the model works equally well for data collected at 435 nm and at 490 nm, but some differences should be noted. Whereas an uncatalyzed pathway contribution is required to fit the data at 435 nm, this term proved insignificant at 490 nm for several of the runs, reducing the model to a three-kinetic-parameter fit. The values obtained for k_c with and without the inclusion of the k_o term are virtually identical at 490 nm. Apparently, the data at 435 nm, because of monomer absorption, expose the formation of the critical nucleus via both pathways, but the data at 490 nm for the J-aggregate

are so dominated by the extended aggregate that large uncertainties exist for the uncatalyzed path. Where estimates can be made at 490 nm for k_0, they center on ~5 × 10^{-5} s^{-1}, which is similar to the value obtained at 435 nm. In general, the pattern observed for the kinetic parameters is 1) $k_c \gg k_o$; 2) m, the size of the critical nucleus is ~5 or 6, with little dependence on starting conditions; and 3) n is ~8 or so, again with little dependence on conditions. The rate constant k_c shows a linear dependence on initial porphyrin concentration, similar to the dependence seen for the *trans*-H_2Pagg/DNA system (Pasternack et al., 1998a).

The values of these kinetic parameters help to account for the rather remarkable sensitivity of the $H_4TPPS_4^{2-}$ aggregation kinetics to the method of preparing solutions. Even when the final concentration conditions are identical, the protocol in which a small volume of a concentrated solution is added to acid leads to appreciably faster kinetics than when the porphyrin is diluted before being acidified. Species are apparently formed in the mixing process which have a significant effect on the kinetics, resulting in hypersensitivity to protocol. We believe that prenuclear species are produced very rapidly as the concentrated porphyrin stock first encounters the aggregating acid medium. These so-called aggregation seeds form and begin the process of aggregation before the solutions can be adequately mixed; that the m value is ~6 implies a very sensitive dependence of the concentration of prenuclear aggregates on total porphyrin concentration, and, as we have already described, k_c, the catalytic rate constant, depends on initial conditions as well. Once a significant concentration of critical nuclei is formed, according to this model, aggregation occurs very rapidly. The result, as seen in Fig. 3, is that the first half-life of a reaction is estimated at ~1000 s for one protocol is less than 10 s for the other.

General comments and applications to other systems

For the two systems considered here, $H_4TPPS_4^{2-}$ and PIC^+, we have observed quite contrasting kinetic profiles, although both chromophores form J-aggregates showing enhanced resonance light scattering signals. Whereas for the latter system, the aggregation is induced by the addition of a polymeric template, this is not likely to be the basis for the difference. It should be recalled that the aggregation of *trans*-H_2Pagg on DNA (Pasternack et al., 1998a) has a kinetic profile similar to that for $H_4TPPS_4^{2-}$. The crucial difference appears to center on whether a rate-determining nucleus formation step is required for aggregation, and whether the aggregate serves as a catalyst for further nucleus formation. For the PIC^+/PVS system, the kinetics can be interpreted as a "simple" assembly of a self-similar fractal object without any need to consider intermediate structures as "bottleneck" steps or catalysis. For $H_4TPPS_4^{2-}$, these considerations are very much involved in the deriva-

TABLE 2 Kinetic parameters, from Eq. 6, for the aggregation of the diacid form of the porphyrin

$[H_4TPPS_4^{2-}]$ (μM)	Wavelength (nm)	k_0 (s^{-1})	k_c (s^{-1})	m	n
2.71	491.5	—	3.3×10^{-4}	5.6	10
3.61	491	—	7.5×10^{-4}	5.0	7.4
3.61	435	4.7×10^{-5}	8.9×10^{-4}	6.1	9.3
4.51	491	4.3×10^{-6}	1.3×10^{-3}	5.3	7.9
5.42	491	3.4×10^{-5}	2.2×10^{-3}	5.9	7.6
5.42	435	2.0×10^{-4}	2.1×10^{-3}	6.5	7.8
6.32	490.5	4.2×10^{-5}	2.9×10^{-3}	5.3	7.4
7.22	491.5	7.9×10^{-5}	3.5×10^{-3}	5.3	8.1

pH 0.5, temperature = 25°C.

tion of the equation used to fit the data. In addition to differences observed in the kinetic profiles, it is important to note the difference in sensitivity of the two systems to the experimental protocol. The detailed analysis of PIC$^+$ aggregation reflects the difficulty in reproducing initial experimental conditions exactly and the small but measurable response of the system to these variations. However, the PIC$^+$ system is relatively insensitive to gross changes in protocol. Not so for the $H_4TPPS_4^{2-}$ system, the half-life of which changes by two or more orders of magnitude, depending on whether concentrated or dilute solutions are mixed to initiate the aggregation process, although the final concentrations are the same. This difference for $H_4TPPS_4^{2-}$, we believe, is closely associated with the requirement for nucleus formation for aggregation to occur. Under the transient conditions of stirring freshly mixed solutions, the rate and extent of nucleus formation do not reflect the equilibrium conditions and have a profound influence on the rate of the aggregation process. If high concentrations of these "aggregation seeds" are produced during the mixing protocol, the aggregation process is enormously enhanced.

It has not escaped our notice that similar processes and sensitivities have been described for biological aggregation processes, such as the recent kinetic data produced by Renault and co-workers for the aggregation of actin (Renault et al., 1999). Actin is a major constituent of muscle cells and has a vital role in numerous cellular functions, such as cell motility, cytokinesis, and phagocytosis. In vivo, monomeric actin, also called G-actin, can reversibly polymerize into microfilaments called F-actin. Previous studies of actin polymerization had been performed in buffering conditions, such that bulk polymerization in the solution generally preceded the surface adsorption of polymers. We have already reported on the applicability of Eq. 6 to these assembly processes (Pasternack et al., 1998a). Surface-induced polymerization from a nonpolymerizing monomer solution was investigated by Renault et. al. This work considered process(es) by which a positively charged lipid monolayer deposited at the air/buffer interface could serve as a template for the polymerization of monomeric actin into single filaments. Under these unique reaction conditions a nucleation period was not observed, unlike in the previously obtained profiles.

Data collected by Renault et al. were scanned; they are presented in Fig. 8 *A*. The authors' analysis was summarized as follows: "the ellipsometric response can be fit with an exponential behavior superimposed on a linear increase that dominated at long times." In other words, two separate phases were used to fit the data; the initial rapid aggregation process was described with a simple exponential function, and a linear function was used to fit the leveling-off portion. Some deviations between the data and the fit are apparent (Renault et al., 1999), particularly at the very early stages of the aggregation and the interface region where the linear equation and exponential function meet. We have attempted
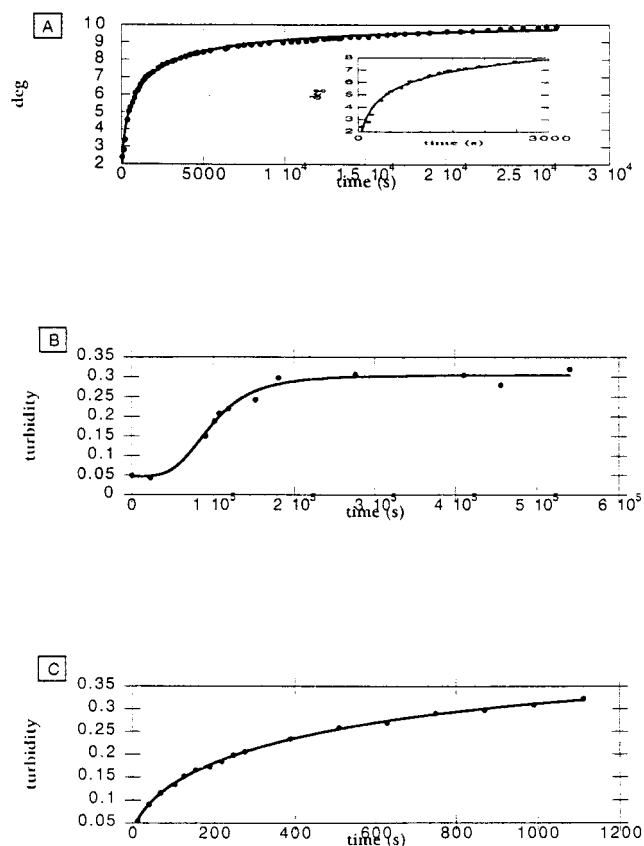

FIGURE 8   (*A*) Refit of actin aggregation data extracted from Renault et al. (1999), using Eq. 5. (*B*) Fit of data provided by Jarrett and Lansbury (1992) for the formation of amyloid fibrils, using Eq. 6. (*C*) Fit to Eq. 5 of data from Jarrett and Lansbury (1992) for the reaggregation of sonicated amyloid fibrils.

to fit the data of Renault et al. with Eq. 5 for a DLA of a fractal object because of the absence of an incubation period. The result is shown in the figure. Although systematic deviations are apparent at long times, the model is quite successful in fitting the vast majority of the aggregation data, and especially the early portions (see *inset*), where the previous model was less successful. As another example of a biologically relevant aggregation, we consider the kinetics of formation of amyloid fibrils investigated by Jarrett and Lansbury (1992). Fibrils, resulting from the aggregation of β-amyloid proteins, are characteristic of the Alzheimer-diseased brain. Jarrett and Lansbury determined that a chemically discriminating nucleation event is necessary for the aggregation of these amyloid proteins. One of the kinetic profiles presented in their paper is reproduced via a scanning routine (described in Materials and Methods) in Fig. 8 *B*. Aggregation was determined as a measure of turbidity of the solution and was initiated by stirring a buffered solution of peptide. The smooth curve shown in the figure was obtained using Eq. 6. The authors then took the product of the kinetic runs, sonicated them to fragment the fibrils
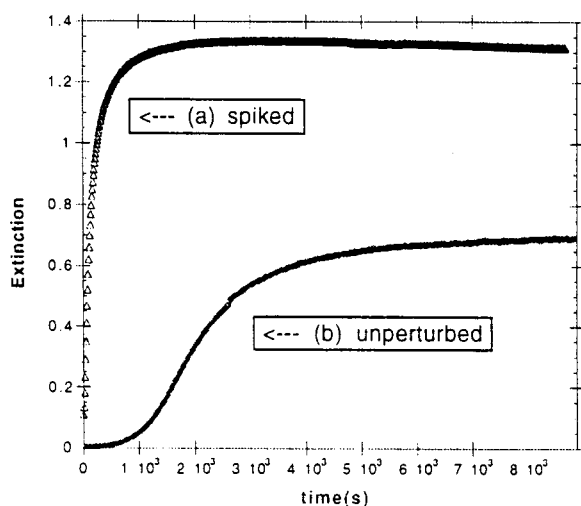
FIGURE 9 The effect of adding "reactive seeds" on $H_4TPPS_4^{2-}$ aggregation kinetics. Curve *a* was obtained for the aggregation process by the addition to a μM $H_4TPPS_4^{2-}$ solution of <100 nM porphyrin from a concentrated stock. Curve *b* is an identical $H_4TPPS_4^{2-}$ solution that was allowed to aggregate without any perturbation.

(ostensibly down to a size characteristic of nucleation sites), and monitored the reformation of fibrils. One of the resulting kinetic profiles is illustrated in Fig. 8C. Note the general similarity in shape to the aggregation profiles of PIC^+ on a PVS template, and the lack of an induction period previously observed for this system (Fig. 8B). The analysis of the Jarrett-Lansbury data using Eq. (5) is shown in the Figure where it can be seen to be quite successful. Clearly the several cases shown in Fig. 8 do not represent a sensitive test for the kinetic models presented here; considerable experimental difficulties limit the precision of the data for these systems. Rather, these analyses are shown to demonstrate the ability of the present models to fit the data for which mechanistic arguments have been made, which are similar to the ones presented here (Jarrett and Lansbury, 1993). To probe still further the parallels between biological aggregations and the those described in the present paper, we attempted a "seeding" experiment with $H_4TPPS_4^{2-}$ to see if it had an impact similar to that observed for β-amyloid. We began two identically mixed aggregation kinetic runs, but "spiked" one with less than 5% (by concentration) of a concentrated $H_4TPPS_4^{2-}$ solution. The impact (see Fig. 9) was remarkable. An incubation period was not observed in the spiked case (Fig. 9, *curve a*), the aggregation kinetics are markedly enhanced, and more porphyrin was converted to aggregate at equilibrium, as compared to the unperturbed kinetic run in curve *b* of Fig. 9. We suggest, therefore, that the kinetic models presented here for relatively simple well-characterized systems provide potentially useful approaches to more complex biologically relevant assembly processes.

REFERENCES

Akins, D. L., H.-R. Zhu, and C. Guo. 1994. Absorption and Raman scattering by aggregated meso-tetrakis(*p*-sulfonatophenyl)porphine *J. Phys. Chem.* 98:3612–3618.

Collings, P. J., E. J. Gibbs, T. E. Starr, O. Vafek, C. Yee, L. Pomerance, and R. F. Pasternack. 1999. Resonance light scattering and its application in determining the size, shape, and aggregation number for supramolecular assemblies of chromophores. *J. Phys. Chem. B.* 103: 8474–8481.

dePaula, J. C., J. H. Robblee, and R. F. Pasternack. 1995. Aggregation of chlorophyll a probed by resonance light scattering spectroscopy. *Biophys. J.* 68:335–341.

Fleischer, E. B., J. M. Palmer, T. S. Srivastava, and A. Chatterjee. 1971. Thermodynamic and kinetic properties of an iron-porphyrin system. *J. Am. Chem. Soc.* 93:3162–3167.

Horng, M.-L., and E. L. Quitevis. 1993. Excited-state dynamics of polymer-bound J-aggregates. *J. Phys. Chem.* 97:12408–12415.

Jarrett, J. T., and P. T. Lansbury, Jr. 1992. Amyloid fibril formation requires a chemically discriminating nucleation event: studies of an amyloidogenic sequence from the bacterial protein OsmB. *Biochemistry.* 31:12345–12352.

Jarrett, J. T., and P. T. Lansbury, Jr. 1993. Seeding "one-dimensional crystallization" of amyloid: a pathogenic mechanism in Alzheimer's disease and scrapie? *Cell.* 73:1055–1058.

Jelley, E. E. 1936. Spectral absorption and fluorescence of dyes in the molecular state. *Nature.* 138:1009–1010.

Leyvraz, F. 1986. Rate equation approach to aggregation phenomena. I*n* On Growth and Form. H. E. Stanley and N. Ostrowski, editors. Martinus Nijhoff Publishers, Dordrecht, the Netherlands. 136–144.

Maiti, N. C., S. Mazumdar, and N. Periasamy. 1998. J- and H-aggregates of porphyrin-surfactant complexes: time-resolved fluorescence and other spectroscopic studies. *J. Phys. Chem. B.* 102:1528–1538.

Maiti, N. C., M. Ravikanth, S. Mazumdar, and N. Periasamy. 1995. Fluorescence dynamics of noncovalently linked porphyrin dimers and aggregates. *J. Phys. Chem.* 99:17192–17197.

Makio, S., N. Kanamaru, and J. Tanaka. 1980. The J-aggregate 5,5′,6,6′-tetrachloro-1,1′-diethyl-3,3′-bis(4-sulfobutyl)benzimidazolocarbocyanine sodium salt in aqueous solution. *Bull. Chem. Soc. Jpn.* 53: 3120–3124.

Norden, B. 1977. Linear and circular dichroism of polymeric pseudocyanine. *J. Phys. Chem.* 81:151–159.

Ohno, O., Y. Kaizu, and H. Kobayashi. 1993. J-aggregate formation of a water-soluble porphyrin in acidic aqueous media. *J. Chem. Phys.* 99: 4128–4139.

Parkash, J., J. H. Robblee, J. Agnew, E. Gibbs, P. Collings, R. F. Pasternack, and J. C. dePaula. 1998. Depolarized resonance light scattering by porphyrin and chlorophyll a aggregates. *Biophys. J.* 74:2089–2099.

Pasternack, R. F., C. Bustamante, P. J. Collings, A. Giannetto, and E. J. Gibbs. 1993. Porphyrin assemblies on DNA studied by a resonance light scattering technique. *J. Am. Chem. Soc.* 115:5393–5399.

Pasternack, R. F., and P. J. Collings. 1995. Resonance light scattering: a new technique for studying chromophore aggregation. *Science.* 269: 935–939.

Pasternack, R. F., L. Francesconi, D. Raff, and E. Spiro. 1973. Aggregation of nickel(II), copper(II), and zinc(II) derivatives of water-soluble porphyrins. *Inorg. Chem.* 12:2606–2611.

Pasternack, R. F., and E. J. Gibbs. 1993. Porphyrin assembly formation on helical biopolymers. *J. Inorg. Organomet. Polym.* 3:77–88.

Pasternack, R. F., E. J. Gibbs, P. J. Collings, J. C. dePaula, L. C. Turzo, and A. Terracina. 1998a. A non-conventional approach to supramolecular formation dynamics. The kinetics of assembly of DNA-bound porphyrins. *J. Am. Chem. Soc.* 120:5873–5878.

Pasternack, R. F., J. I. Goldsmith, S. Szep, and E. J. Gibbs. 1998b. A spectroscopic and thermodynamic study of porphyrin/DNA supramolecular assemblies. *Biophys. J.* 75:1024–1031.

Pasternack, R. F., P. R. Huber, P. Boyd, G. Engasser, L. Francesconi, E. Gibbs, P. Fasella, G. C. Venturo and L. deC. Hinds. 1972. On the aggregation of meso-substituted water soluble porphyrins. *J. Am. Chem. Soc.* 94:4511–4517.

Pasternack, R. F., K. F. Schaefer, and P. Hambright. 1994. Resonance light scattering studies of porphyrin diacid aggregates. *Inorg. Chem.* 33:2062–2065.

Renault, A., P.-F. Lenne, C. Zakri, A. Aradian, C. Venien-Bryan, and F. Amblard. 1999. Surface-induced polymerization of actin. *Biophys. J.* 76:1580–1590.

Ribo, J. M., J. Crusats, J.-A. Farrera, and M. L. Valero. 1994. Aggregation in water solutions of tetrasodium diprotonated meso-tetrakis(4-sulfonatophenyl)porphine. *J. Chem. Soc. Chem. Commun.* 681–682.

Rubires, R., J. Crusats, Z. El-Hachemi, T. Jaramillo, M. Lopez, E. Valls, J. A. Farrera, and J. M. Ribo. 1999. Self-assembly in water of the sodium salts of meso-sulfonatophenyl substituted porphyrins. *New J. Chem.* 189–198.

Scheibe, G. 1936. Variability of the absorption spectra of some sensitizing dyes and its cause. *Angew. Chem.* 49:563.

Sundstrom, V., T. Gilbro, R. A. Gadonas, and A. Piscaska. 1988. Annihilation of singlet excitons in J aggregates of pseudoisocyanine (PIC) studied by pico- and subpicosecond spectroscopy. *J. Chem. Phys.* 89:2754–2762.